JOINT EUROPEAN TORUS

JET–P(87)46

T.P. Hughes and S.R.P. Smith

Calculations of Thomson Scattering Functions for Alpha Particle Diagnostics in JET Plasmas

Calculations of Thomson Scattering Functions for Alpha Particle Diagnostics in JET Plasmas

T.P. Hughes and S.R.P. Smith

JET-Joint Undertaking, Culham Science Centre, OX14 3DB, Abingdon, UK

Preprint of Paper to be submitted for publication in
Nuclear Fusion

ABSTRACT. Scattering functions are calculated for conditions anticipated for DT plasmas in JET. It is concluded that scattering at millimetre wavelengths may be capable of providing useful information about the alpha-particle velocity distribution function, whereas scattering of CO_2 laser radiation at a wavelength of 10.6 μm will not. Significantly lower values are found at 10.6 μm than those published by Vahala *et al*. The alpha distribution function is most easily determined when the geometry is such as to minimize the effect of the plasma magnetic field.

1. INTRODUCTION

There is currently considerable interest in the possibility of using a Thomson scattering technique to determine the velocity distribution of contained alpha-particles from DT reactions in high-temperature Tokamak plasmas. An intense, coherent radiation source is required. Hutchinson *et al*. [1] proposed the use of a carbon dioxide laser at a wavelength of 10.6 μm, while Woskoboinikow [2] has suggested the use of a gyrotron with a wavelength of a few millimeters.

The spectrum of the scattered radiation can be calculated for a given velocity distribution of alpha-particles if the plasma parameters and the scattering geometry are known. Following preliminary calculations by Hutchinson *et al*. [1] in which the effects of magnetic fields were ignored, Vahala, Vahala and Sigmar (Ref. [3] – henceforth referred to as VVS) presented formulae for the calculation of scattering spectra together with some computed spectra relevant to CO_2 laser scattering in magnetised plasmas.

In the present paper, these calculations have been extended, with significant corrections, to other scattering wavelengths. It is shown, for typical JET plasmas, that it is not feasible to use CO_2 laser scattering as an alpha-particle diagnostic. On the other hand, we find that the use of gyrotron radiation is more promising, though it will still be necessary to take into account additional considerations, including refraction, signal-to-noise ratio and access to the plasma, which are outside the scope of this paper. It is also shown that the effects of the magnetic field can be almost eliminated and the interpretation of the scattering spectrum consequently greatly simplified by arranging for the scattering wavevector to be at a sufficiently large angle to the magnetic field direction.

2. THEORETICAL FORMULATION

The theoretical formulation of the present calculations for electromagnetic scattering in plasmas follows that of VVS [3], based on the description by Sheffield [4] (see also references cited therein). We repeat only the bare outline of this work.

The power scattered into solid angle $d\Omega$ with bandwidth $d\omega$ at frequency ω from length L of a beam of power P_I in a plasma of electron density n_e is given by

$$P_S \, d\Omega \, d\omega = P_I \, \Gamma r_0^2 n_e L \; S(\underline{k},\omega) \, d\Omega \, d\omega$$

where $r_0^2 = 8\times10^{-30}$ m^2, $S(\underline{k},\omega)$ is the scattering function and Γ is a geometrical factor of order unity which takes into account the polarization of the radiation (see Bretz [5]). The scattering wave vector $\underline{k}$ is given, for incident and scattered wave vectors $\underline{k}_I$ and $\underline{k}_S$, by

$$\underline{k} = \underline{k}_S - \underline{k}_I \; ,$$

and $$|\underline{k}| \equiv k = 2 \, k_I \sin(\theta/2) \; ,$$

where θ is the scattering angle between $\underline{k}_I$ and $\underline{k}_S$. The direction of $\underline{k}$ is taken to lie at an angle φ to that of the magnetic field $\underline{B}$.

We shall consider here only the fundamental problem of calculating the scattering function $S(\underline{k},\omega)$ in a plasma containing one or more species (i) of ions and some alpha-particles. We may write

$$S(\underline{k},\omega) = S_e(\underline{k},\omega) + \sum_i S_i(\underline{k},\omega) + S_\alpha(\underline{k},\omega) \; ,$$

where $S_e(\underline{k},\omega)$ is the electron scattering function, $S_i(\underline{k},\omega)$ the scattering due to the electrons dressing the ions (of number density n_i, charge Z_i and mass M_i), and $S_\alpha(\underline{k},\omega)$ the corresponding alpha-particle scattering function. The electrons and ions are assumed to have Maxwellian energy distribution functions with effective temperatures T_e and T_i (defined such that $k_B T_j$ gives the mean kinetic energy $m_j v_j^2/2$, j = e or i). $S_e(\underline{k},\omega)$ is given by

$$S_e(\underline{k},\omega) = |1 - H_e/\epsilon_L|^2 \, \frac{2\pi^{1/2}}{|k_\parallel| v_e} \, F_1(x_e, w_e, W_e) \; ,$$

where

$$F_1(x,w,W) = \sum_{m=-\infty}^{\infty} e^{-x} \, I_m(x) \, \exp\{ -(w-mW)^2 \}$$

$$x_e = (k_\perp v_e/\Omega_e)^2/2 \; , \quad w_e = \omega/k_\parallel v_e \; , \quad W_e = \Omega_e/k_\parallel v_e \; .$$

Ω_e is the electron cyclotron frequency, and $k_\parallel$ and $k_\perp$ are the scattering wavevector components parallel and perpendicular to the magnetic field. The longitudinal dielectric function ϵ_L is

$$\epsilon_L(\underline{k},\omega) = 1 + H_e(\underline{k},\omega) + \sum_i H_i(\underline{k},\omega) + G_\alpha(\underline{k},\omega) ,$$

with

$$H_e(\underline{k},\omega) = \alpha^2 \, \mathbb{Z}(x_e,w_e,W_e) .$$

Here, the Salpeter parameter $\alpha = 1/|\underline{k}|\lambda_D$, the Debye length $\lambda_D = v_e/2^{1/2}\omega_{pe}$, and the electron plasma frequency $\omega_{pe} = (n_e e^2/m_e\epsilon_0)^{1/2}$. The function

$$\mathbb{Z}(x,w,W) = [1 - 2wF_2(x,w,W) + i\pi^{1/2} F_1(x,w,W)]$$

where

$$F_2(x,w,W) = \sum_{m=-\infty}^{\infty} e^{-x} \, I_m(x) \, D(w-mW)$$

and D(z) is Dawson's integral

$$D(z) = \exp(-z^2) \int_0^z \exp(p^2)dp .$$

Similarly, the 'magnetised' ion dielectric function is

$$H_i(\underline{k},\omega) = \alpha^2(Z_i^2 n_i T_e/n_e T_i) \, \mathbb{Z}(x_i,w_i,W_i)$$

with number density n_i and Maxwellian temperature T_i. The alpha-particles are assumed to be 'unmagnetised', in the sense that they do not complete a cyclotron orbit within the scattering volume. With an alpha-particle velocity distribution function $f_\alpha(\underline{v})$, G_α is given by

$$G_\alpha(\underline{k},\omega) = (\omega_{p\alpha}/k)^2 \int d^3v \; \underline{k}.\frac{\partial f_\alpha(\underline{v})}{\partial \underline{v}} \; \frac{1}{(\omega - \underline{k}.\underline{v} + i\delta)} .$$

The ion scattering function is given by

$$S_i(\underline{k},\omega) = |H_e/\epsilon_L|^2 \; \frac{2\pi^{1/2} Z_i^2 n_i}{n_e|k_\parallel|v_i} \; F_1(x_i,w_i,W_i) ,$$

and the alpha-particle function by

$$S_\alpha(\underline{k},\omega) = |H_e/\epsilon_L|^2 \; \frac{2\pi Z_\alpha^2 n_\alpha}{n_e|\underline{k}|} \; f_\alpha^{(1)}(\omega/k) ,$$

where the one-dimensional distribution function $f_\alpha^{(1)}$ for alpha-particle velocity $v_{\parallel}$ along the direction of $\underline{k}$ is

$$f_{\alpha}^{(1)}(v_{\parallel}) = \int d^2\underline{v}_{\perp}\; f_{\alpha}(\underline{v}) \;.$$

VVS originally used the 'unmagnetised' shielding electron response, and in their expression (17) for $S_{\alpha}(\underline{k},\omega)$ the factor $|H_e/\epsilon_L|^2$ was replaced by $|\alpha^2[1 + \zeta_e\{i\pi^{1/2}\exp(-\zeta_e)-2D(\zeta_e)\}]|^2$ with $\zeta_e=(\omega/kv_e)$, but G. Vahala has pointed out (private communication) that the assumption of the 'magnetised' shielding response is more appropriate.

For f_{α} we use the "slow-down" form given by VVS:

$$f_{\alpha}(\underline{v}) = \begin{cases} 0 & , \quad v > v_{\alpha} \\ F_0/(v^3 + v_c^3) & , \quad v < v_{\alpha} \end{cases}$$

where $F_0 = 3/[4\pi\, \ell n(1+v_{\alpha}^3/v_c^3)]$, $v_c \simeq 0.09v_e$, $v_{\alpha} = (2E_{\alpha}/M_{\alpha})^{1/2}$ and the energy of the alpha-particles at birth is $E_{\alpha} = 3.5$ MeV (so $v_{\alpha} = 1.3\times10^7$ m s^{-1}). This leads to the expression for the one-dimensional distribution function

$$f_{\alpha}^{(1)}(u) = (-2\pi F_0/3v_c)\left[\frac{1}{2}\ell n\left\{\frac{(y+v_c)^2}{y^2-v_cy+v_c^2}\right\} - 3^{1/2}\tan^{-1}\left\{\frac{2y-v_c}{3^{1/2}v_c}\right\}\right]_{y=u}^{y=v_{\alpha}}$$

in which a correction has been made to the upper evaluation limit given by VVS.

3. NUMERICAL PROCEDURE

The principal computational task is the evaluation of summations of the form

$$F_i(x,w,W) = \sum_{m=0}^{\infty} e^{-x}\, I_m(x)\; f_m^i(w,W)$$

where $I_m(x)$ is the modified Bessel function of order m, and

$$f_m^i(w,W) = \exp[-(w-mW)^2] + \exp[-(w+mW)^2] \quad \text{for } i=1,\ m\neq0,$$

$$= \exp[-w^2] \qquad \text{for } i=1,\ m=0,$$

$$= D(w-mW) + D(w+mW) \qquad \text{for } i=2,\ m\neq 0,$$

$$= D(w) \qquad \text{for } i=2,\ m=0.$$

The Bessel functions obey the recursion relations

$$(2m/x)\ I_m(x) = I_{m-1}(x) - I_{m+1}(x) \ .$$

Although polynomial approximations for $I_0(x)$ and $I_1(x)$ are well known, upward recursion is unstable for the large m-values required here. The sums F are therefore evaluated using a Clenshaw type of algorithm, which uses a downward recursion method (see Press *et al*, [6]). The quantities

$$A_n = (1/I_n)\sum_{m=n+1}^{\infty} I_m f_m \ , \quad B_n = (1/I_n)\sum_{m=n+1}^{\infty} I_m \quad \text{and} \quad R_m = I_m/I_{m-1}$$

are defined, which obey the recursion relations

$$A_{n-1} = R_n(f_n+A_n) \ , \quad B_{n-1} = R_n(1+B_n), \text{ and } \quad R_n = 1/[(2n/x)+R_{n+1}\ ].$$

These are evaluated with n decreasing from an initial value N, taking $A_{N+1}=R_{N+1}=B_{N+1}=0$. Using the Bessel function normalisation condition

$$1 = \sum_m e^{-x} I_m(x)$$

one evaluates the summations as

$$F_i = (A_0^i + f_0^i)/(1 + 2B_0) \ .$$

The F_i are evaluated using an initial value for N of $\text{Int}[(40x)^{1/2}+10]$ and a re-evaluation using $N\to 1.5N$ to check that a relative accuracy of 10^{-7} is obtained. In the most stringent case, the evaluation of these summations requires N-values of up to around 500 for the ion function F_2 at an incident wavelength of $\lambda_I=10.6\ \mu m$.

The other computational task of note is the evaluation of Dawson's integral D(z). For $0\leq z\leq 3.9$, the integral is evaluated by interpolation from a tabulated look-up table, whilst for $z>3.9$, the polynomial approximation given by Abramowitz, Milton and Stegun [7] is used.

4. CALCULATED DATA

The standard plasma conditions used in computing the spectra are:

T_e = 10.00 keV, n_e = 1.200x10^{20} m^{-3},

T_i = 20.00 keV, n_i = 1.185x10^{20} m^{-3}, Z_i=1, M_i=2.5,

n_α = 7.500x10^{17} m^{-3}, Z_α=2, M_α=4,

B = 3.4 T,

and in the slow-down distribution, $v_c = 0.09\ v_e$.

In some cases, two or three species of plasma ion are included, and in all cases, charge neutrality is assumed: i.e.

$$n_e = \sum_i Z_i n_i + Z_\alpha n_\alpha \ .$$

Access for gyrotron radiation to the centre of the plasma in JET is possible for the conditions specified at frequencies near 140 GHz in the O-mode (between the fundamental and the second harmonic of the electron cyclotron frequency Ω_e) or near 60 GHz in the X-mode (below the cyclotron fundamental and above the right hand cut-off). Both these frequencies have been considered.

Calculated spectra are given in Figs. 1-6, and show both the total scattering function $S(\underline{k},\omega)$ and the background (ion + electron) scattering S_b=S-S_α as functions of frequency $\nu = \omega/2\pi$. The ion scattering dominates at low frequencies (up to around 1 GHz), the alpha contribution extends up to the cut-off frequency ω_α=v_α k , and the electron response is dominant thereafter. At small $k_{\parallel}$ ($\varphi \simeq$ 90°), the lower hybrid resonance becomes prominent. The approximate frequency of this resonance in a cold plasma (as given by VVS) is:

$$\omega^2 = \left\{1 + \frac{m_i k_\parallel^2}{m_e k_\perp^2}\right\} \frac{\omega_{pi}^2}{1 + \omega_{pe}^2/\Omega_e^2} \quad .$$

its computed position (defined as that frequency ν_{LH} at which there is a zero, or failing that a minimum, in the real part of the dielectric function ϵ_L) is marked by an arrow in the Figures.

Figs. 1 and 2 show the results of calculations for CO_2 radiation. The ratio S_α/S_b in the region of the alpha-particle feature can be made reasonably large only if the Salpeter parameter $\alpha \geqslant 2$. At 10.6 μm this can be achieved for JET plasmas only when $\theta \leqslant 0.7°$. Fig. 1 shows the relative growth of the alpha-particle signal as θ decreases in the 'non-magnetic' case $\varphi=0$: the ratio S_α/S_b would increase further for even smaller angles θ, but this would require an angular resolution that is likely to be unattainable experimentally. The ratio S_α/S_b also varies rapidly with φ as $\varphi\to 90°$, when the lower hybrid resonance occurs within the alpha-particle feature, as shown in Fig.2. Near to ν_{LH}, the total signal is enhanced, but as this is primarily due to an increase in S_b, the ratio S_α/S_b is reduced. At frequencies well above ν_{LH}, S_b is very small and the alpha-particle scattering can be entirely dominant (as seen in Fig. 2 when $\varphi=89°$ and partially when $\varphi=87°$), but S is then actually less than in the $\varphi=0$ case. It is also apparent from Fig. 2 that the spectra change rapidly with φ when φ-90°, and it appears that the experimental resolution necessary in order to extract data of a quality satisfactory for alpha-particle diagnostics is again unlikely to be attainable. Thus, in attempting to determine $f_\alpha(\underline{v})$ there is no advantage to be gained by making measurements in the region of ν_{LH}.

We conclude that CO_2 radiation (λ_I = 10.6 μm) is not suitable for alpha-particle diagnostics in JET plasmas. It should be noted that our calculated values for S are considerably lower than those of VVS, a discrepancy that can only in small part be attributed to the modifications made here to their formulae.

Figs. 3 to 6 show data appropriate to 140 and 60 GHz gyrotron sources. At these frequencies, which are much lower than that of CO_2 laser radiation, the Salpeter parameter α is always greater than 2 for the plasma conditions assumed, the ratio S_α/S_b is large and the scattering geometry is therefore far less restricted. We give a detailed discussion of the Figures 3-6 below:

Fig. 3 shows θ = 90° scattering for φ = 0°,85°,89° and 89.8°. There is little difference between the φ=0° and φ=85° spectra (though the background S_b is greater in the latter case). The lower hybrid resonance becomes prominent for φ = 89.0° and 89.8°, and considerable magnetic structure becomes apparent in the latter case. The detailed magnetic structure is unlikely to be experimentally resolvable for two reasons. Firstly, the formalism used actually gives zero damping at φ=90°, where the scattering wave vector is exactly perpendicular to the magnetic field, and so this formalism must in principle be modified for $\varphi \simeq 90°$. Secondly, the resolved magnetic structure is in any case an artefact introduced by having a single ion species, and is substantially modified and complicated when two or more species of ion are present (see the discussion of Fig. 4 below). Thirdly, any experimental observation will include a range of φ, thereby smearing out the detail.

Fig. 4 shows the effect of including two species of ion, with equal densities of ions of masses $M_{i1} = 2$ and $M_{i2} = 3$ (both with $Z_i = 1$) replacing the single ion of average mass $M_i = 2.5$. This has little effect except close to the "fully magnetised" case $\varphi \simeq 90°$. The spectra are shown at 60 GHz for $\varphi=89.8°$ and $\theta=90°$, where the well-defined ion resonance structure observed in the average ion case becomes in the two-ion case very complex and doubtless experimentally unresolvable.

Fig. 5 shows the effect of varying the overall densities n_i, n_e and n_α together by factors of 2 or ½ from the standard conditions. Away from the ion feature, the basic shape of the alpha contribution is virtually unaffected by these variations. The differences can be mainly accounted for by the variation in the Salpeter parameter α (which conditions the electron response), as is clearly apparent above the alpha cut-off frequency $\omega_\alpha \sim 3.2$ GHz. We have also checked that the scattering response is similarly insensitive to changes in the electron and ion temperatures T_e and T_i away from the ion feature, and also to the effects of introducing up to 10% of ^{12}C impurity ions ($Z_i=6$, $M_i=12$).

Fig. 6 demonstrates the effect of modifying the slow-down distribution function $f_\alpha(\underline{v})$ by changing the parameter v_c (by factors of 2 and ½) in order to gain some feel for the sensitivity of this type of experiment to the details of the alpha-particle energy distribution function. The results are shown on both logarithmic (Fig. 6(a)) and linear (Fig. 6(b)) scales.

5. DISCUSSION

The aim of this work has been to identify some experimental conditions under which a Thomson scattering experiment can in principle provide useful information about the alpha-particle velocity distribution in JET.

The principal competitors as a radiation source are at present a CO_2 laser or a gyrotron operating at 140 GHz or 60 GHz (in regions of low plasma emission). The preference is for the gyrotron source. At 10.6 μm the spectrum changes very rapidly with angle, only small angle scattering can be used, and there is nothing to be gained from utilising the lower hybrid resonance. In contrast, at gyrotron frequencies, much larger scattering angles are available, the spectra change only slowly with angle, and reasonably large collection solid angles can be used — limited possibly by coherence requirements for heterodyne detection.

Assuming that a gyrotron source is used, the insensitivity of the spectra to scattering geometry away from the lower hybrid resonance makes it sensible to use φ-values $\lesssim 80°$. The avoidance of the resonance condition, whilst reducing the signal strength, has the advantage that a much truer representation of the alpha-particle distribution function can be directly obtained from the experimental data. When magnetic effects are small ($\varphi \lesssim 80°$), it is readily shown that the spectrum of radiation scattered from the alpha-particles, in the region outside the plasma ion feature, is approximately given by

$$S_\alpha(\underline{k},\omega) \approx \frac{8\pi n_\alpha}{k n_e} f_\alpha^{(1)}(\omega/k)$$

$$= \frac{2\lambda_I n_\alpha}{\sin(\theta/2) n_e} f_\alpha^{(1)}(\omega/k) \ .$$

When $S_\alpha \gg S_b$, as is usually the case at mm wavelengths in this region of the spectrum, $S(\underline{k},\omega) \simeq S_\alpha(\underline{k},\omega)$, and so $f_\alpha^{(1)}(\omega/k)$ is immediately obtainable from the observed scattered spectrum. Thus, for example, under the conditions used for Figure 5, the values of S calculated from the above expression are within 5% of the accurate computed values between 1.1 and 3.0 GHz.

The choice of angle θ will depend primarily on considerations outside the scope of this paper, including for example the effects of refraction and the availability of ports for the incident and scattered beams. Considerations of source power and detector design are also beyond the scope of this paper. Nonetheless, preliminary estimates suggest that although the scattering functions calculated here are small, the extraction of the alpha-particle distribution function from Thomson scattering experiments may be possible using existing technology.

ACKNOWLEDGEMENTS

This work was performed under contract with the JET Joint Undertaking. The authors are indebted to A. E. Costley, D. Bartlett, J.A. Hoekzema and C. Gowers of JET for many discussions, and to G. Vahala for a communication.

REFERENCES

[1] HUTCHINSON,D.P.,VANDERSLUIS,K.L.,SHEFFIELD,J.,SIGMAR,D.J., Rev. Sci. Instrum. 56 (1985) 1075.

[2] WOSKOBOINIKOW, P., COHN, D.R., MACHUZAK, J.S., TEMKIN, R.J., Massachusetts Institute of Technology Plasma Fusion Center Report PFC/CP-86-16 (1986).

[3] VAHALA, L.G.,VAHALA,G.,SIGMAR,D.J., Nuclear Fusion 26 (1986) 51.

[4] SHEFFIELD,J., *Plasma Scattering of Electromagnetic Radiation*, Academic Press, New York (1975).

[5] BRETZ, N., *Geometrical Effects in X-mode Scattering*, Princeton Plasma Physics Laboratory Report, PPPL 2396 (Oct. 1986).

[6] PRESS,W.H.,FLANNERY,B.P.,TEUKOLSKY,S.A.,VETTERLING,W.T., *Numerical Recipes*, Cambridge University Press, Cambridge, UK (1986).

[7] ABRAMOVITZ,MILTON,STEGUN,I.A.,*Handbook of Mathematical Functions*,Applied Mathematics Series, vol. 55, National Bureau of Standards, Washington (1964).

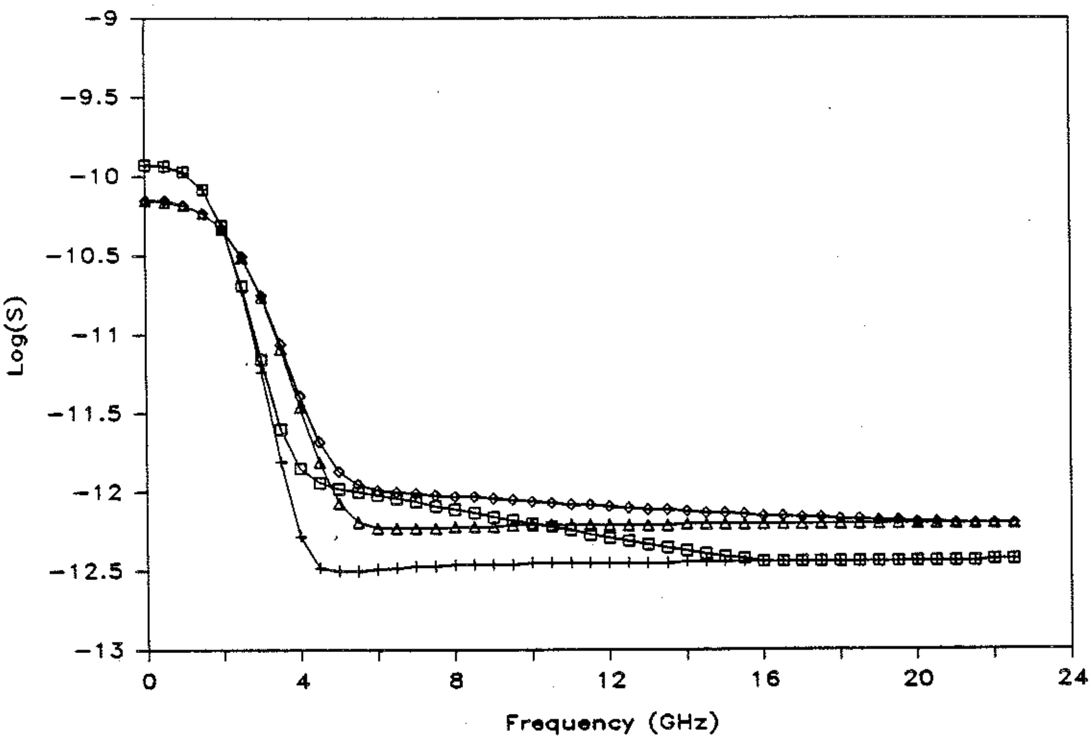

Figure 1. $S(\underline{k},\omega)$ and $S_b(\underline{k},\omega)$ for CO_2 laser radiation (λ_I=10.6 μm) at φ=0, with θ=0.75° (□ symbol for S; + for S_b) and θ=1.0° (◊ for S; △ for S_b).

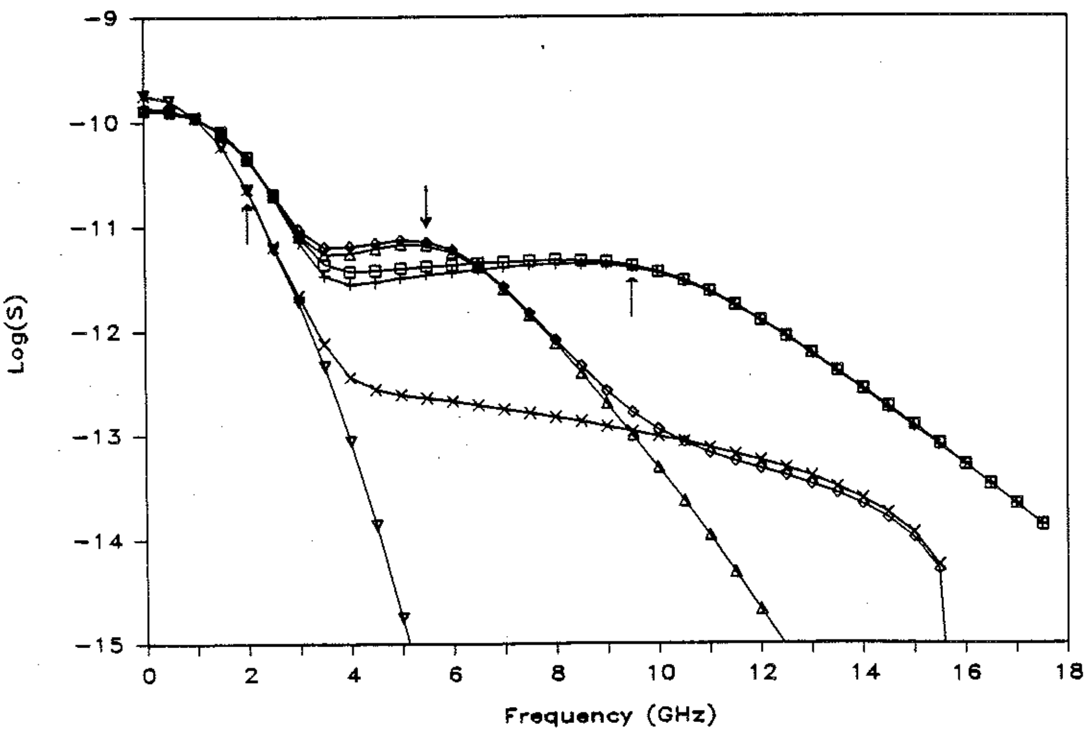

Figure 2. $S(\underline{k},\omega)$ and $S_b(\underline{k},\omega)$ at λ_I=10.6 μm at θ=0.75°, with φ=85° (□ for S_t; + for S_b), φ=87° (◊ and △) and φ=89° (✗ and ▽).

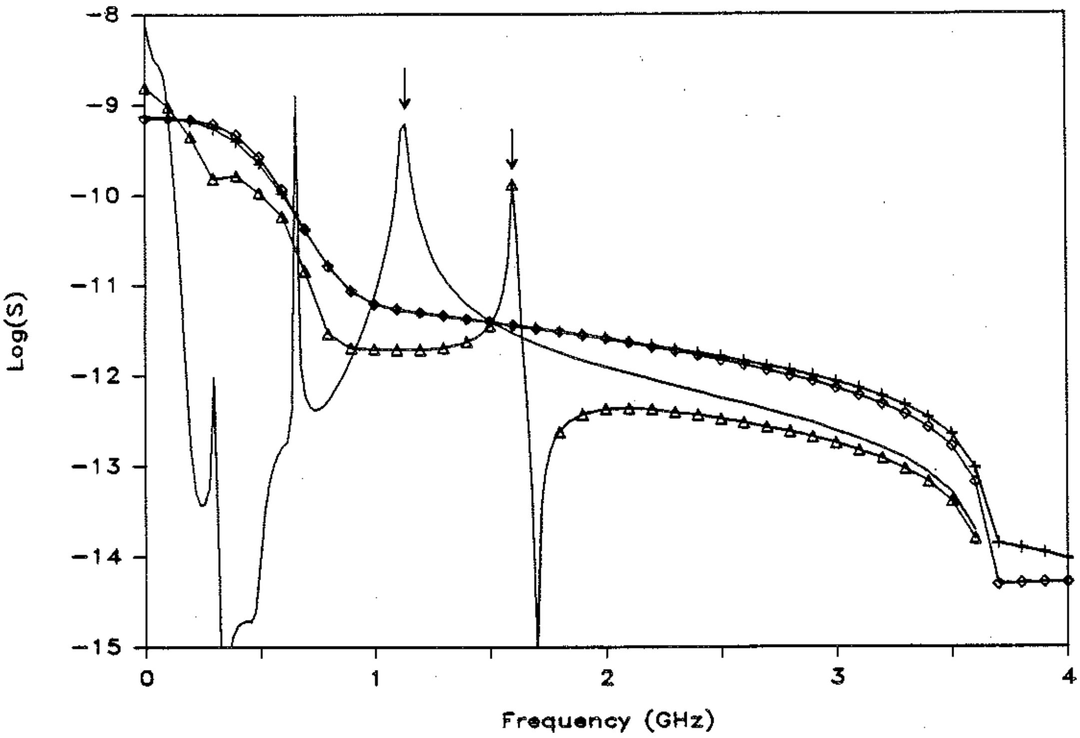

Figure 3. S($\underline{k}$,ω) for gyrotron radiation at ν_I=60 GHz at θ=90°, with φ=0.0° (◊), 85.0° (+), 89.0° (△) and 89.8° (-).

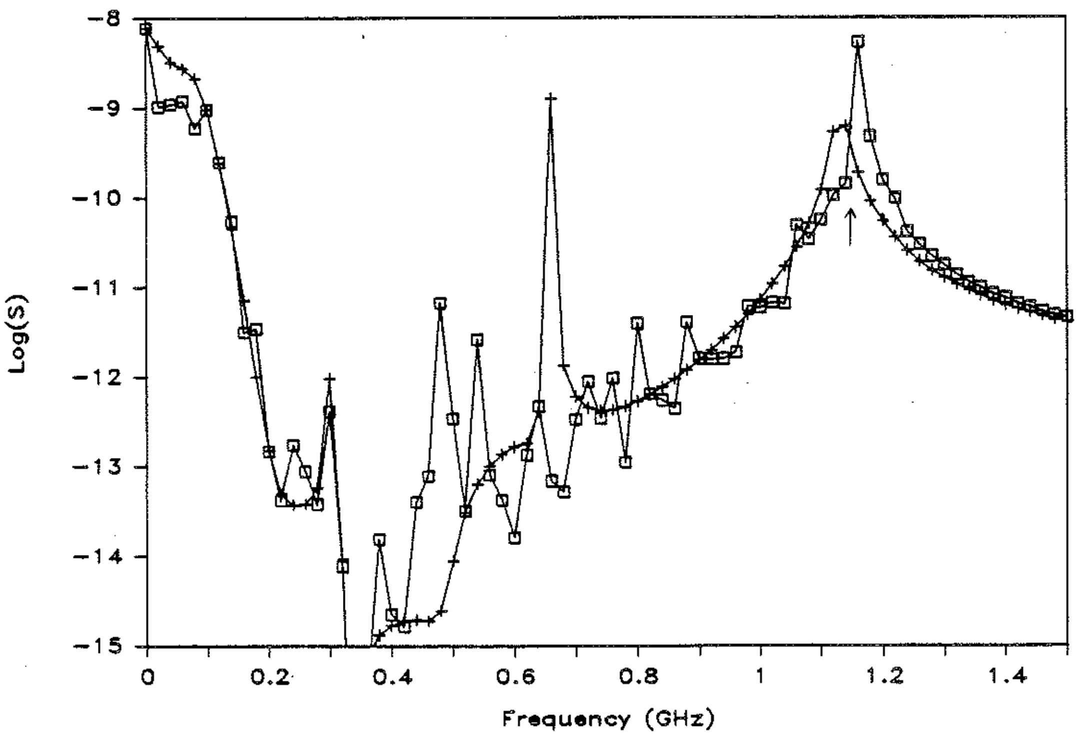

Figure 4. S($\underline{k}$,ω) at ν_I=60 GHz with θ=90° and φ= 89.8°, showing the single average ion response M =2.5 (+) and the two-ion response M_{i1}=2, M_{i2}=3 (□).

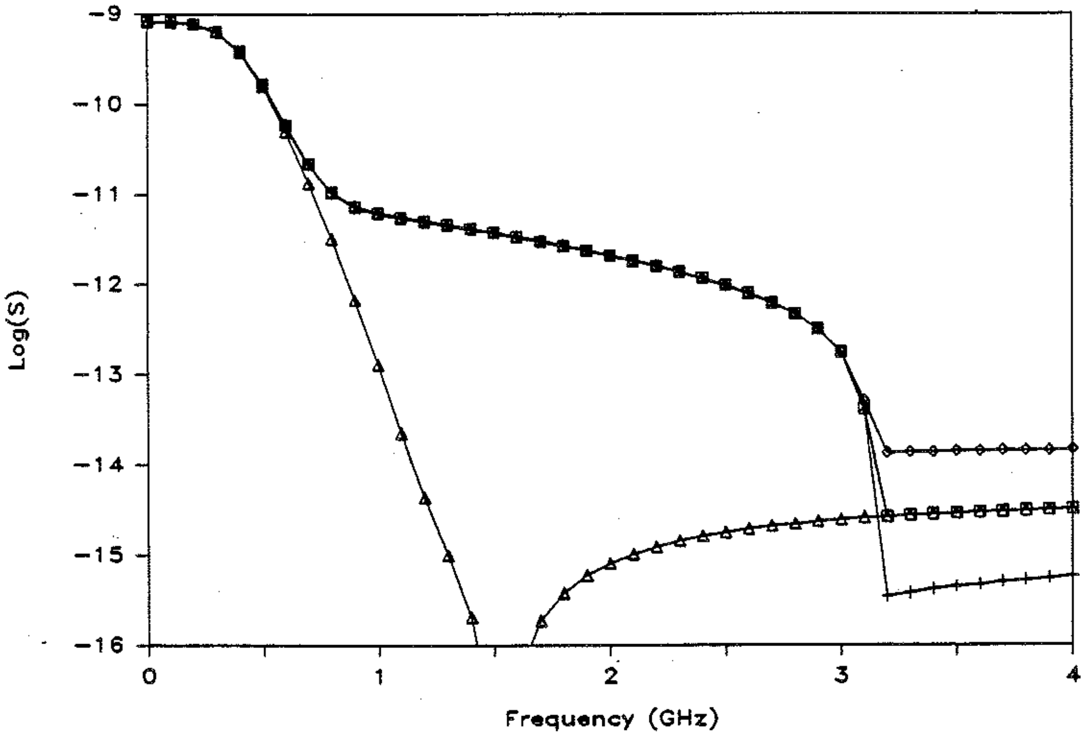

Figure 5. $S(\underline{k},\omega)$ at ν_I=140 GHz with θ=30° and φ=0°, showing the effect of multiplying the standard particle densities n_e, n_i and n_α by: 1 (□) [together with the background S_b (△)]; 2 (+); ½ (◇).

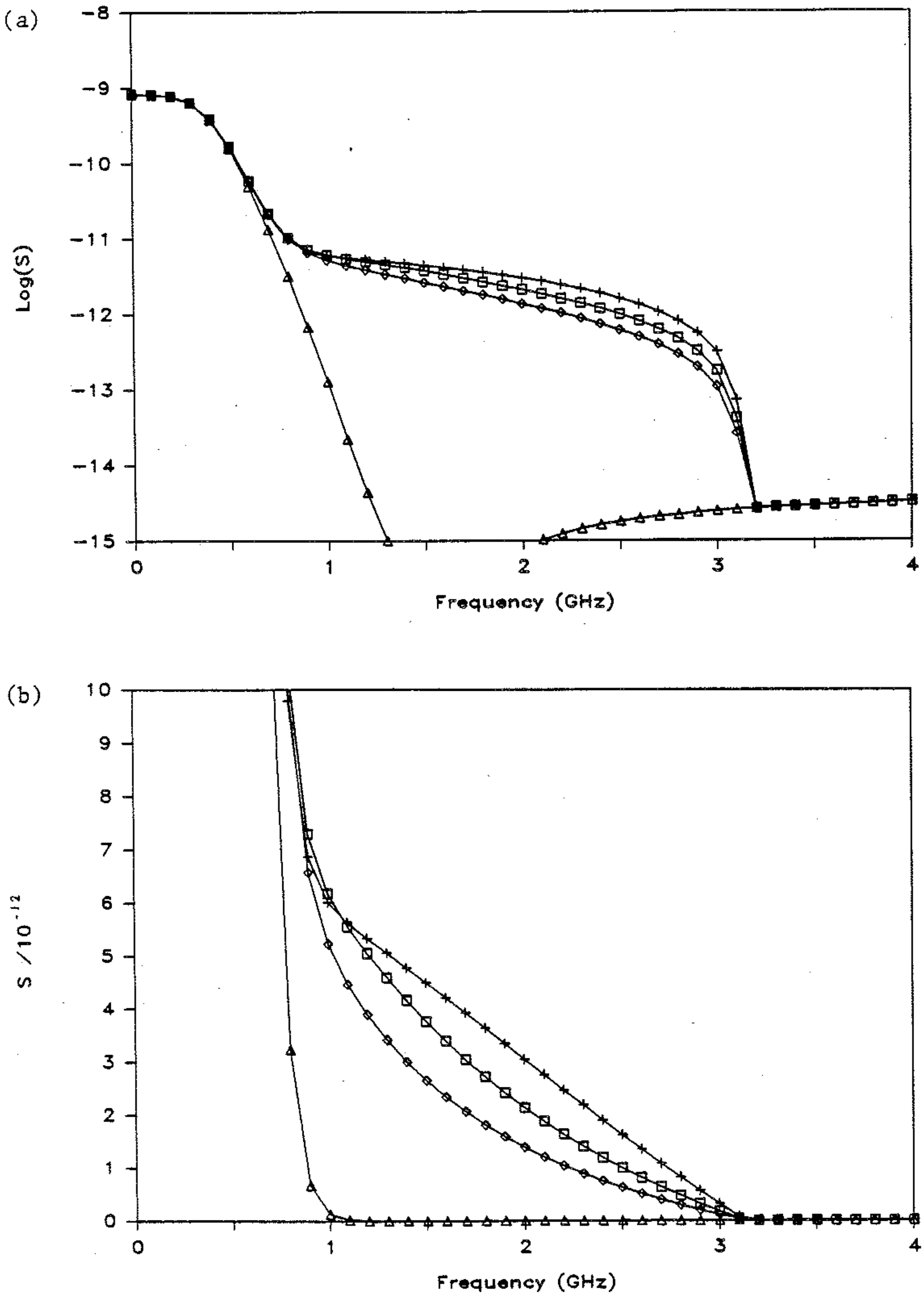

Figure 6. $S(\underline{k},\omega)$ at ν_I=140 GHz with θ=30° and φ=0°, with the following values of v_c/v_e in the slow-down distribution function: 0.09 (□) [together with the background S_b (△)]; 0.18 (+); 0.045 (◊): (a) logarithmic scale, and (b) linear scale.